STEADILY DISCHARGING ECCENTRIC WELLS: COMPARING NUMERICAL SIMULATIONS TO EXISTING EXPERIMENTS

Sevgi Cavdar
Assistant Professor, Department of Civil Engineering, Faculty of Engineering, Sivas Cumhuriyet University, Sivas, Turkey
Abdusselam Altunkaynak
Professor in Civil Engineering Department, Civil Engineering Faculty, Istanbul Technical University, Istanbul, Turkey.
Hasan G. Elmazoghi
Department of C.E., Faculty of Engineering, University of Benghazi, Benghazi, Libya
https://doi.org/10.5281/zenodo.18631633

Abstract

Operation of eccentric wells in a circular island unconfined aquifer under steady state flow conditions was addressed in this study by comparing the results of experimental, analytical and developed numerical models. MODFLOW was used in the developed numerical models. The results include simulations of various refined meshes. Such relationships are of practical importance in operating eccentric wells in unconfined radial flow systems. The objectives of this study were: 1) to determine the drawdown ranges, in terms of their agreement, among the numerical, experimental, and analytical solutions; 2) to test whether the MODFLOW (using PCG2 and PCGN solvers) provides accurate results for such wells; and 3) to investigate the sensitivity of the numerical solutions to mesh size and eccentricity. The results showed that all solutions performed better for smaller drawdowns in eccentric wells than they do for larger drawdowns; and for smaller drawdowns, analytical and PCG2 models provided good agreement taking into consideration root-mean-square error as evaluation criteria. For larger drawdowns, analytical and PCG2 either grossly overestimated the drawdown values or became inapplicable as the hydraulic head in well dropped to zero. PCGN solver performed best for both smaller and larger drawdowns, but the parameter selection needs care. Eccentricity and mesh size have effects on the solutions, especially for parameter estimation in PCGN, and the consistency of outputs requires investigation of optimal mesh size depending on eccentricity. When compared to wells with larger eccentricity, linear PCGN (PCGN1) performed better for large eccentricity regardless of mesh size, while PCG2 performed better for wells closer to the concentric. Numerical methods predicted larger drawdowns for finer mesh spacing size. Based on these results, numerical solutions could be used to adequately describe the drawdown for a well placed eccentrically within a circular island unconfined aquifer under steady state flow conditions provided the modeling parameters are dealt with scrutiny.

Keywords: Drawdown, Eccentric well, Unconfined circular aquifer, Numerical model

Introduction

Hantush and Jacob (1960) conducted a theoretical study under steady state flow conditions for a discharging well located eccentrically in a circular confined aquifer along whose outer cylindrical boundary either the drawdown or the flux is zero. De Wiest (1963) performed an analytical solution for the flow to an eccentric well in a leaky circular aquifer with lateral replenishment, for both steady and unsteady flow conditions. Later on, Verruijt (1982) developed a theoretical equation for the wells eccentrically located in an unconfined circular aquifer under steady state flow conditions. Birpinar and Gazioglu (2002) performed an experimental study for wells located eccentrically in an unconfined aquifer with finite extent to test the validity of the equation presented by Verruijt (1982); they concluded that the Verruijt (1982) equation is valid for small drawdowns. According to Mishra and Kuhlman (2013), despite the many advanced solution methods available, there exists still a need for realism to simulate real-world aquifer tests accurately.

In this study, Processing MODFLOW (which uses structured rectilinear grids mesh) was adopted to simulate the wells eccentrically located in a circular island unconfined aquifer. For MODFLOW solutions and, the sensitivity of the solution to mesh size and eccentricity was investigated by changing the regional and local grids. A comparison was performed with the experimental results of Birpinar and Gazioglu (2002) and the analytical solution of Verruijt (1982). A priorly developed FORTRAN Code (FC) by the last author that uses finite difference method was also adopted for comparison purposes.

The objectives of this study were to determine the drawdown ranges where the mentioned solution methods approximate the experimental and/or each other; to investigate the sensitivity of the numerical solutions to mesh size; and to test whether the MODFLOW (using PCG2 and PCGN solvers) provided accurate results for wells eccentrically located in unconfined circular aquifer under steady state flow conditions. Based on the comparison of these solution methods, the drawdown and the discharge-drawdown relationship at the well in operation under different discharge rates were predicted. Understanding such relationships is of practical interest in operating unconfined radial flow systems. It was assumed that the aquifer is homogeneous, the wells are unlined and fully penetrated the aquifer thickness, Darcy's law is valid for the flow in the aquifer, and only one well is pumped at a time using a constant discharge rate until equilibrium conditions occur.

Model of the study

To have a direct, logical and easy comparison between the results of the available experimental and analytical solutions with MODFLOW, the considered flow domain was discretized in a way that the wells are placed at locations within the aquifer as those in Birpinar and Gazioglu (2002) experiments (Fig. 1). The performances of all models were compared for the same soil properties, problem dimensions and flow geometry. The physical experimental study was constructed using a sand model contained in a square box. The thickness of the circular aquifer model was 50 cm. The boundary condition head in the sand model was kept constant at about 7 cm below the sand surface. In brief, the constant values for the applied circular aquifer model were taken as: H = 42.8 cm (referred to the base of the aquifer), k = 0.468 cm/s, r_w =1.75 cm and r = 96 cm, where H is the height of initial water table, k is the permeability of the unconfined aquifer, r_w is the well radius, and r is the radius of the aquifer (radial distance from the center of the aquifer to its external circular boundary).

Analytical solution

Using the image well theory, Verruijt (1982) developed an analytical equation for a sink ($+Q$) placed eccentrically at $x = p$, $y = 0$ as shown in Fig. 2, where p is the well eccentricity. The problem was solved by inserting a source ($-Q$) at $x = r^2/p$, $y = 0$, where both sink and source were operating in an infinite circular unconfined aquifer. With application of appropriate boundary condition, Verruijt obtained that:

$$h_w^2 - H^2 = \frac{Q}{\pi k}\ln\left(\frac{r_w r}{r^2 - p^2}\right) \quad (1)$$

When the eccentricity $p = 0$, Eq. (1) reduces to Dupuit's expression derived by integrating Darcy's law for steady flow around a well in a homogeneous and isotropic unconfined aquifer.

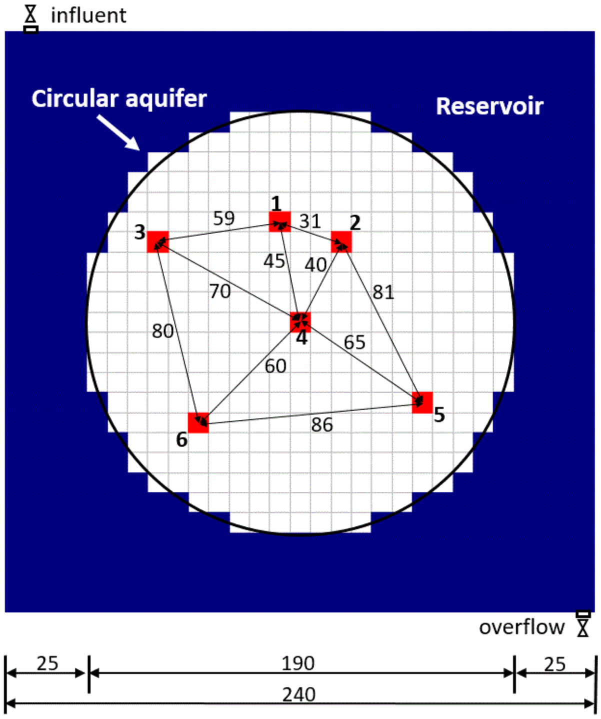

Fig. 1 Well locations in a 29x29 global grid system, units in cm. Red squares represent the wells with their numbers.

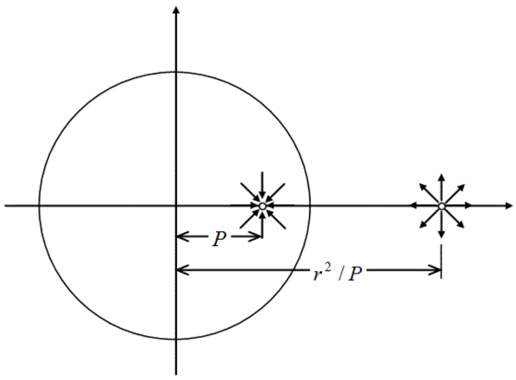

Fig. 2 Schematic sketch with sink and source for Verruijt analytical solution

Governing equation & boundary conditions

With MODFLOW-2005, using block centered flow package, unconfined layer property and well package under MODFLOW model, the problem at hand was solved using PCG2 and PCGN solvers. Some results were compared to finite difference method results conducted using Fortran Code (FC) prior to this work. The code solved Eq.(2) using Gauss-Seidel iteration with successive over-relaxation. The equation provides the two-dimensional model for incompressible steady groundwater flow in a homogeneous unconfined aquifer and was formulated introducing Dupuit's assumption that head, h, does not vary in the vertical direction (i.e., $\partial h / \partial z = 0$) resulting in horizontal flow (Wang and Anderson, 1982).

$$\frac{\partial^2 v}{\partial x^2} + \frac{\partial^2 v}{\partial y^2} = -\frac{2R(x,y)}{k} \quad (2)$$

where $v = h^2$, $R(x,y)$ is the volume of water recharged per unit time per unit aquifer area and $R(x,y) = Q / \Delta x \Delta y$, where Q is the discharge rate from the well and k is the hydraulic conductivity. Those results are used to make partial comparison to MODFLOW results.

Dirichlet boundary condition was considered in this study for MODFLOW (and FC). That is, the head is known (h = constant = 42.8 cm) for all the nodal points on the outer circular boundary of the flow region and remains unaffected for distances greater than the radius of the aquifer. In FC, the solution of these equations were first obtained in terms of (v) and the head (h) at all nodal points were then obtained by taking into consideration the square root of v. Previous researches by Boulton (1951), Hantush (1964), and others proved by mathematical procedures that the discharge obtained by introducing the Dupuit assumption represents a correct solution even though the water table obtained by the same procedure, known as Dupuit parabola, significantly deviates from the real water table, especially where the streamlines are strongly curved. According to Clement et al. (1996), the deviation from Dupuit discharge is within 1 to 2 %. Shamsi and Narasimhan (1991) suggested that the Dupuit model underestimates the discharge because the flux through the seepage face is ignored and the deviation may range up to 10 to 12 %. Siddiraju (2013) concluded that the specific capacity of open wells increases as the diameter of the well increases.

MODFLOW

Well locations (eccentricity), discharge rates, and domain mesh (both regional and local) are the varying concepts in both the FC and MODFLOW models. The Pickard iteration number, however, is only introduced to MODFLOW models. Simulations were done using various uniform grids to which, later, local refinement was also applied. Preconditioned Conjugate-Gradient solvers PCG2 and PCGN (MODFLOW-2005) with parameters in Table 1 were used to solve the matrices. All parameters were kept constant except one of the three outer iteration number (*iter_mo*) in PCGN. The linear solution was obtained using *iter_mo* 1, and the converged result was obtained by picking a high number—100. An extra step was then considered to test the possibility of obtaining a meaningful output by restricting the iteration number.

Table 1 Parameters used A) in PCG2 solver and B) in PCGN in MODFLOW

A) PCG2

Preconditioning method		**Allowed Iteration #**		**Convergence Criteria**		**Damping**
	Relaxation Parameter	Outer Iteration	Inner Iteration	Head Change (cm)	Residual (cm^3/s)	Damping Parameter
MIC	.99	50	30	.001	.001	1

B) PCGN

Preconditioning method	**General Solver Parameters**					**Damping**	**Convergence of Inner Iteration**
	Relaxation Parameter	Outer Iteration	Inner Iteration	Residual CLOSE_R	Head Change (CLOSE_H)	Damping Parameter	ACNVG
MIC	.99 | 0 fill	1|TBD| 100	500	.001	.001	ADAMP: 0 DAMP: .5	0

To decide the optimal *iter_mo* with the model at hand (beside 1 and 100), its effects on discharge and on well location were analyzed (Fig. 3). Discharge magnitude had almost no effect on *iter_mo* (Fig. 3a); thus, a single *iter_mo* can be chosen for a well pumped with various discharges (e.g. nine is representative enough for well 4). Our analyses showed that well location does require increasing *iter_mo*s as the distance from the constant head boundary becomes larger (Fig. 3b). There is an optimal *iter_mo* below and above which the solutions are not as close to the experimental study. This, however, is only a problem faced with larger discharge rates. With lower discharge rates, the simulations provide robust outputs. For identifying *iter_mo*s in PCGN solver, if no observation data is available, the following procedure may be applied: analytical and numerical solutions already provide comparable results for the center well, from which one can identify the ideal *iter_mo* for the model by adjusting *iter_mos*. For a trend to be obtained, a second *iter_mo* at another location is needed, which could be the one at the outer boundary where the *iter_mo* functions close to unity. The only exception to increasing *iter_mo* concept is well 5; its results mimic that of well 1. It should be noted that the experimental model gives completely different discharge-drawdown relationships than any of the analytical equation or the developed numerical models for well 5. Its relation should be between those of wells number 6 and 3, but it does not. Birpinar and Gazioglu (2002) repeated their experimental work, but the result of well 5 did not change. This is not the case with any of the analytical or the numerical results, which give correct behaviors as expected for all wells when their eccentricity is considered. The pronounced deviations in the experimental results and the different behavior of well 5 may suggest that the experimental model requires sensitivity analysis to changes in the well radius and model size. Its closeness to the overflow or remoteness to the inflow in the sand tank could be another explanation to this.

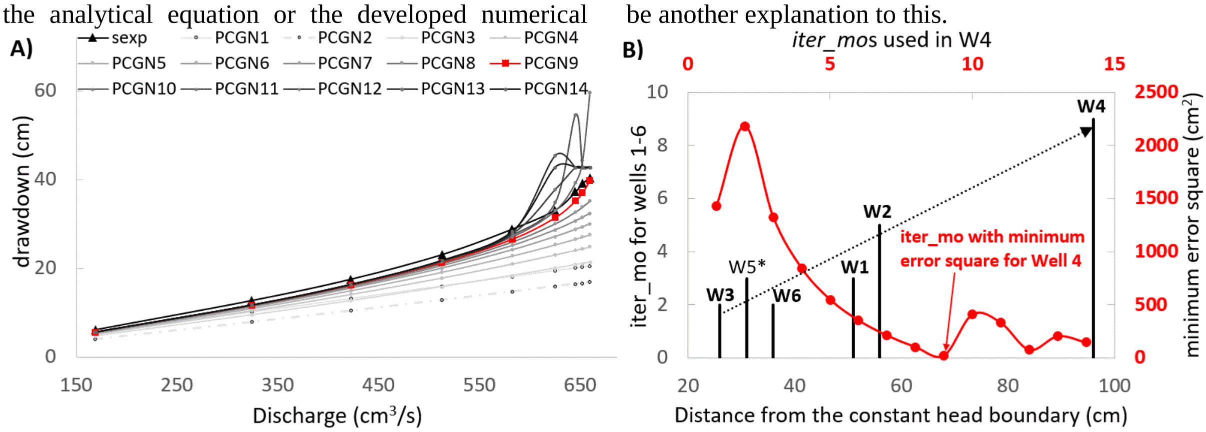

***Fig. 3** Deciding optimal iter_mo: a) results obtained using different iter_mos for all discharge rates applied to well 4 (experimental drawdowns in black triangles and best match in red squares); and b) the optimal iter_mos.*

Four different uniform global grids were applied to the study area for MODFLOW and FC (Table 2), finest approximately having the area of wells constructed in the experimental model. For MODFLOW only, each global system was refined at and around the wells (Table 2).

Table 2 A) Four different global meshes, showing the number of layers, rows, and columns before and after refinement; B) visualization of (A) in close proximity to the well in operation, extracted from MODFLOW.

A)	**Layers, Rows, Columns**		
Discretization	**Pre-refinement (FC & MODFLOW)**	**Refinement I (MODFLOW Only)**	**Refinement II (MODFLOW Only)**
Case I	1, 25, 25	1, 31, 31	1, 37, 37
Case II	1, 29, 29	1, 35, 35	1, 41, 41
Case III	1, 51, 51	1, 57, 57	1, 63, 63
Case IV	1, 77, 77	1, 83, 83	1, 89, 89
B) Changes with refinement in well cell(s) (in red) and the first four neighboring cells in the lower right-hand portion of wells	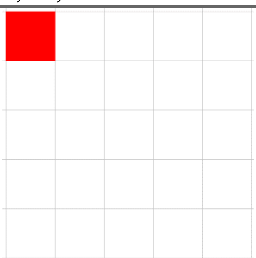	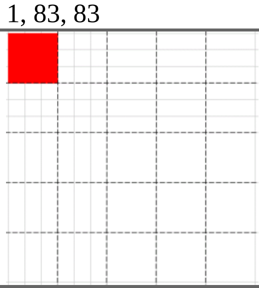	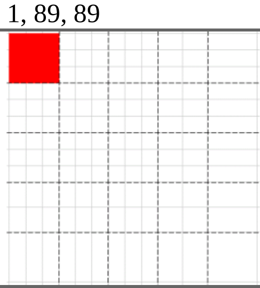

Referred to as *refinement I* and applied to each well position in all global systems, the eight cells enclosing the well in global grid system was refined by inserting two rows and two columns, thereby splitting each mentioned global cell into nine cells (Table 2). To avoid the refinement of one well affecting the mesh of other wells, *Refinement I* was implemented in different MODFLOW models for each well. In *refinement II*, applied only to Well 1 in all four global grids, variable spacing employed. In *refinement I*, only the first neighboring cells were used enclosing the well; in *refinement II*, second and third neighboring cells were also added to the first. Adding two columns and two rows applied to the first and second neighboring cells, and only one column or one row was added to the third—thus the name variable.

Table 3 A rough flow chart with the corresponding model names in MODFLOW. n varies with each well.

DEFINITION / FLOW	**MODEL NAME**		
	Refinement at the well	**Solver**	***Iter_mo***
• Form a uniform grid in MODFLOW • Pick a well and locate its position • Run simulations for all experimental discharge rates	 non-refined	PCGN ↑ Solver	1 | n | 100 ↑ Iter_mo
• Apply refinement I and • average the drawdowns of nine small wells • Run simulations for all experimental discharge rates	R 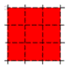 Refinement I	PCGN ↑ Solver	1 | n | 100 ↑ Iter_mo
• Use single refined center cell (only applied to well 1) • Run simulations for all experimental discharge rates	SCWR 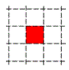 Refinement I	PCGN ↑ Solver	1 | n | 100 ↑ Iter_mo
• Apply refinement II (only applied to well 1) • average the drawdowns of nine small wells • Run simulations for all experimental discharge rates	R2 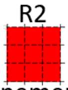 Refinement II	PCGN ↑ Solver	1 | n | 100 ↑ Iter_mo

In all local refinements, there was peripheral refinement in that the rows and columns added extend throughout the model domain. Therefore, while it would be expected, for example, the third neighboring cells divided into two, in MODFLOW, they are divided into six cells due to the refinement of closer neighboring cells to the well-corner cells split into four with intersection of third neighboring cells' refining column and row. Because of this, the well itself too, in all refined models, were divided into nine cells (Table 3). The focus in local refinement was on obtaining detailed information about large hydraulic gradients and on getting results that represents the reality (i.e. experimental results) better. The well area was kept as in the global grid, and the pumping rates were scaled by the cell area, dividing the discharge by 9. The sum of the pumping rates (and the area) remain the same as that of the global single-cell well. Only for Well 1 was the well area changed by a factor of nine, using a single-cell after applying *refinement I* (SCWR in Table 3).

Analyses of the results

The experimental and the analytical drawdowns were drawn in Fig. 4. Analytical model considerably overestimates the drawdowns for all wells except Well 4.

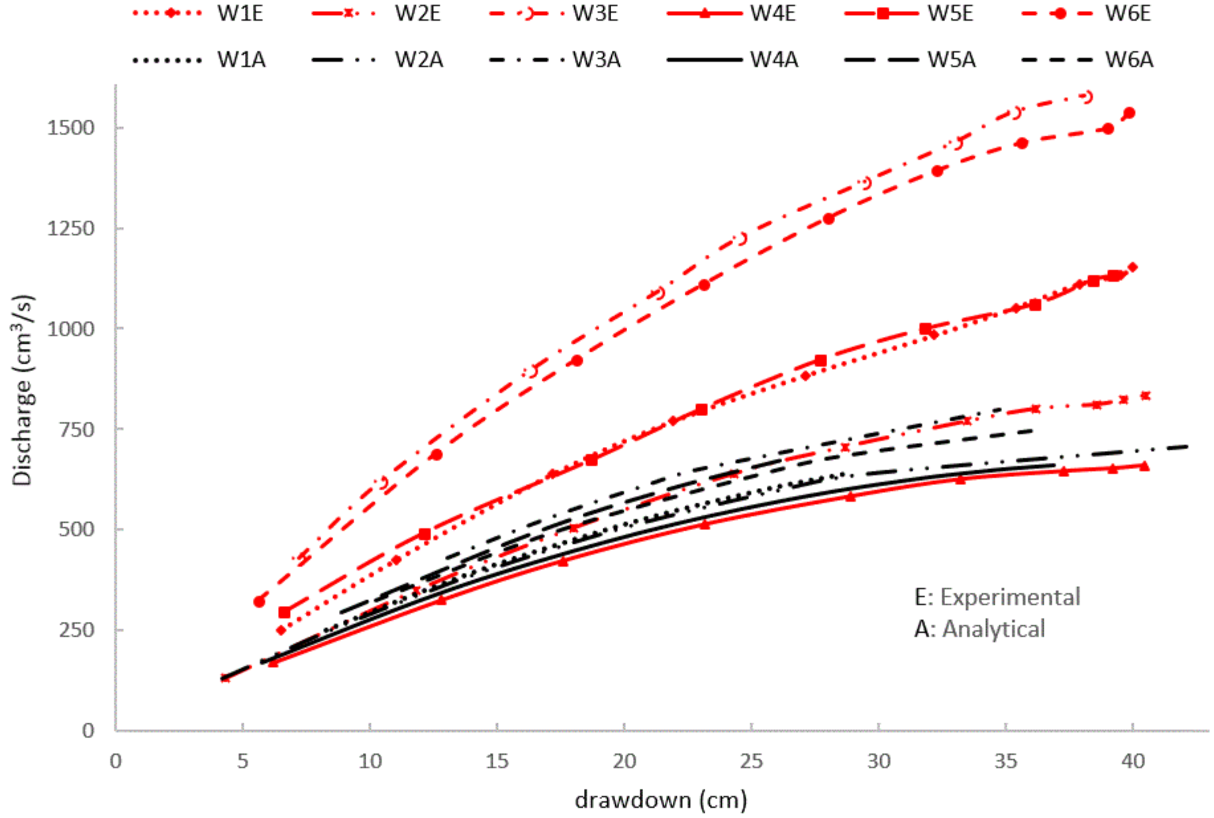

Fig. 4 Discharge-drawdown relationship from experimental and analytical models for wells 1 to 6

Table 4 shows the percentage differences in Well 1 for *case I* discretization (similar calculations and discharge-drawdown relationships were obtained for all wells). The differences between the experimental and analytical, and experimental and numerical results were considerable and mostly increase as the discharge rates increase. Consistent decrease takes place for PCGN1 and SCW RPCGN1; however, it is only for PCGN1 that the decrease is meaningful with a range from 11.4% to 1.6%. PCGN3's percentage difference, on the other hand, differs in that, first an increase and then a decrease takes place, which is promising for the accuracy of larger discharge rates. Difference for SCW models results are almost double. Interestingly, for 769.2 cm^3/s, models with *refinement I* and *refinement II* seem to plateau with an average difference of 17.9%. For FC, the difference increases as the discharge rate increases. Because PCG2 results replicated the results of PCGN100, they were omitted from the study altogether. Similarly, analytical, FC, and PCGN100 results almost overlap, producing similar errors when compared with the experimental model.

Table 4 Smaller drawdown values of well 1, corresponding to the smallest 4 of 10 discharge rates applied in the experimental model. For model names, refer to Table 1; NA symbolizes that the model does not provide any drawdown because the head reaches the bottom of the well with a lower discharge rate. For numerical solutions, case I mesh is applied.

Q (cm^3/s)	**250.2**	**425.4**	**638.4**	**769.2**
Experimental drawdown, s (cm)	6.5	11.05	17.2	21.9
Analytical drawdown, s0 (cm)	8.3	15.5	28.7	NA
Error % between s & s0	27.2	40.4	66.6	
FC drawdown, s1 (cm)	8.0	14.9	27.0	NA
Error % between s & s1	22.8	34.9	56.8	
PCGN1 drawdown, s2 (cm)	7.2	12.3	18.5	22.3
Error % between s & s2	11.4	11.4	7.4	1.6
PCGN3 drawdown, s3 (cm)	6.7	11.8	18.9	23.7
Error % between s & s3	2.6	7.1	9.6	8.4
PCGN100 drawdown, s4 (cm)	8.0	15.0	NA	NA
Error % between s & s4	23.0	35.93		
RPCGN1 drawdown, s5 (cm)	5.9	10.0	15.0	18.0
Error % between s & s5	9.7	9.7	12.9	17.6
RPCGN3 drawdown, s6 (cm)	5.3	9.4	14.7	18.2
Error % between s & s6	17.8	15.2	14.7	16.9
RPCGN100 drawdown, s7 (cm)	6.3	11.5	19.4	26.1
Error % between s & s7	2.5	4.3	12.6	19.2
R2PCGN1 drawdown, s8 (cm)	5.8	9.9	14.9	17.9
Error % between s & s8	10.3	10.3	13.6	18.2
R2PCGN3 drawdown, s9 (cm)	5.3	9.3	14.6	18.1
Error % between s & s9	18.4	15.8	15.3	17.4
R2PCGN100 drawdown, s10 (cm)	6.3	11.4	19.2	25.8
Error % between s & s10	3.2	3.5	11.6	18.0
SCW RPCGN1 drawdown, s11 (cm)	9.5	16.1	24.2	29.1
Error % between s & s11	45.7	45.7	40.5	32.9
SCW RPCGN3 drawdown, s12 (cm)	8.9	16.0	26.2	34.0
Error % between s & s12	36.3	44.4	52.3	55.3
SCW RPCGN100 drawdown, s13 (cm)	10.9	21.9	NA	NA
Error % between s & s13	67.1	97.7		

Root mean-square errors ($RMSE$) were calculated for each well using drawdown differences between Birpinar and Gazioglu (2002) measurements and those obtained from the developed numerical models for all four grid cases (Table 5). In order also to consider the effect of discharge rate magnitude, first, the smallest two discharge rates and their corresponding drawdowns were combined ($RMSE_1 = \sqrt{\frac{\sum_{i=1}^{2}(s_{ip}-s_{ia})^2}{2}}$, where s_{ip} and s_{ia} are the calculated and the experimental drawdowns, respectively). Second, all discharge rates, large and small, for which the drawdowns obtained were used (i.e. the well does not become dry applying that discharge rate on the numerical solution; $RMSE_2 = \sqrt{\frac{\sum_{i=1}^{n}(s_{ip}-s_{ia})^2}{n}}$). Some methods produce results for high discharge rates for the same well (and grid) while others do not; results were also affected by the global grid and local refinements. For example, for 29x29 grid (*case II)*, well 2 operates for a maximum discharge of 504 cm^3/s for PCGN100 model, while the same well runs for the 833.4 cm^3/s and still provides a hydraulic head of 17.3 cm for PCGN1 method. For 77x77 grid (*case IV*), well 2 becomes dry before reaching a discharge of 504 cm^3/s—if refinement is applied, discharge rates go up to 769.2 cm^3/s for PCGN100 (i.e. RPCGN100) and the well still does not become dry.

Table 5 $RMSE$ obtained using drawdowns from numerical and experimental models for all four grid cases. For each column, the first value is for the small drawdown (maximum drawdown of 11.8 cm, using first two discharges applied to the well.

		FC (cm)		MODFLOW (cm)											
				PCGN1		PCGNn		PCGN100		RPCGN1		RPCGNn		RPCGN100	
Case I	W1	2.9	6.1	1.0	4.1	0.6	1.7	3.0	3.0	0.9	8.8	1.4	6.8	0.4	3.5
	W2	0	3.9	1	10.3	0	0	0	1	2.4	13.9	2.2	9.8	1.7	8.6
	W3	8.2	8.2	4.6	5	1.7	1.7	8.8	8.8	1.7	3.3	0	6.2	3.6	6
	W4	1	3.7	2	12.6	1	1.7	1	1	3.5	15.4	2.6	11.3	2.6	11
	W5	2.8	7.1	1	5.9	0	2.6	3	6.2	1.4	10.4	2	9.7	0	5.6
	W6	11.1	11.1	4.9	5.3	2	2.2	4.3	4.3	2	3.6	0	6.3	5	9.7
Case II	W1	3.5	7.3	1.4	3.5	1	2.6	3.6	3.6	0	7.7	1	5.4	1	3
	W2	0	3	1	9.8	0	0	0	1.5	2.2	13.3	2	8.8	1.4	7.3
	W3	8.7	9.3	4.8	5.5	2	2.2	9.3	9.3	1.7	3	0	5.7	3.9	6.9
	W4	0	2	1.7	12.2	0	1	0	0	3.2	15.1	2.4	10.6	2.4	10.3
	W5	3.3	10.1	1.4	4.7	1	1	3.9	3.9	1	9.2	1.4	8.1	0	4.5
	W6	14.4	14.4	5.2	5.8	2.2	2.8	4.6	4.6	2.2	3.3	0	5.7	5.5	26.7
Case III	W1	6	6	3.0	2.8	2.6	6.4	6.2	6.2	1	4	0	1	3	6.7
	W2	2.2	4.5	0.4	6.9	1.4	6.2	2.2	5.2	1	10.3	0.5	2.6	0.2	4.5
	W3	14.1	14.1	7.3	10.8	4.1	7.4	9.1	9.1	4.4	4.7	1.6	1.5	8	9.4
	W4	1	5.8	0	9.8	1	2.8	**4.7**	**4.2**	2	12.6	1	5.1	1	6.9
	W5	6.6	14.1	3.2	2.6	2.8	5.1	6.9	6.9	1	5.7	0	3	3	5
	W6	6.7*	6.7	7.8	11.2	4.6	7.9	6.7*	6.7	4.9	5.2	2	2	11.3	11.6
Case IV	W1	8.1	8.1	4.2	5.5	3.9	9.6	8.3	8.3	2.2	2.2	1.7	4.6	4.8	7.5
	W2	3.5	7.2	1.2	3.7	2.4	7.5	3.6	3.6	0.2	8.2	0.6	3.2	1.3	3.1
	W3	20	20	9.1	13.3	5.6	9.9	11.5*	11.5	6.2	8.4	3.1	4.8	11.4	13.2
	W4	2.3	6.2	0.4	8.2	2.2	6.2	2.4	4	1.2	11	0.2	1	0.3	5.8
	W5	9.2	9.2	**4.5**	**3.7**	4.2	7.9	9.8	9.8	2.2	3.3	1.8	2	5.1	6.3
	W6	8.2	8.2	9.6	13.2	6.2	9.6	8.3	8.3	6.6	9.3	3.5	5.5	12.2	12.2

Aiming to decide which method provides better results and with which grids, we observed another parameter taking a role in conclusions: the eccentricity-distance of the well to the concentric well. Because of this, while comparing the methods; we looked into the effect of well location with respect to the distance from the center of the circular aquifer. The FC performs best for the center well and the wells closer to it when compared to the wells a far from the aquifer center; so does the analytical solution. As the wells get farther from the center and closer to the specified boundary, the FC results diverge further from the experimentals for a single operating well. *Case II* grid is optimal for the center well, and closest to it, well 2; as the distance from the center increases, finer global grids (*case III*) work better, but for wells too close to the boundary, none is appropriate that there may be an optimal grid somewhere between 29x29 and 51x51 (Table 5; refer to Fig. 1 or 3b for eccentricity).

PCGN1, the linear solution, provides good results overall for wells 1 and 5, regardless of grid size. PCGN100, which is the converged case without local refinement, produces better results regardless of the global grid when the wells located within the inner part of the aquifer diameter, and as far as $RMSE$s are concerned, *case I* provides better approximations. Nonetheless, for PCGN100, MODFLOW provides outputs only for the smaller discharges used in Birpinar and Gazioglu (2002) study, meaning PCGN100 grossly overestimates the drawdowns (except for well 4 in coarser grids), so the number of outputs included for the wells is fewer comparing with other methods used in MODFLOW.

PCGNn functions well in general, but coarser grids provide even better results; maximum $RMSE$ for *case I* is 2.6 cm (Fig. 5a). For finer global grids, the results using mentioned *iter_mo*s do not show any success unless local refinement is applied. RPCGNn, which is the latter mentioned case, produces overall the best predictions for finer global grids; Wells 1, 2, 3, and 6 are better with *case III*, 4 and 5 with *case IV* (Fig. 5B). Considering Well 5, which has high systematic errors in the experimental model, it could be stated that, for eccentric wells, *case III* is the optimal grid among the ones tested in this study using RPCGNn (Table 5; Fig. 5b).

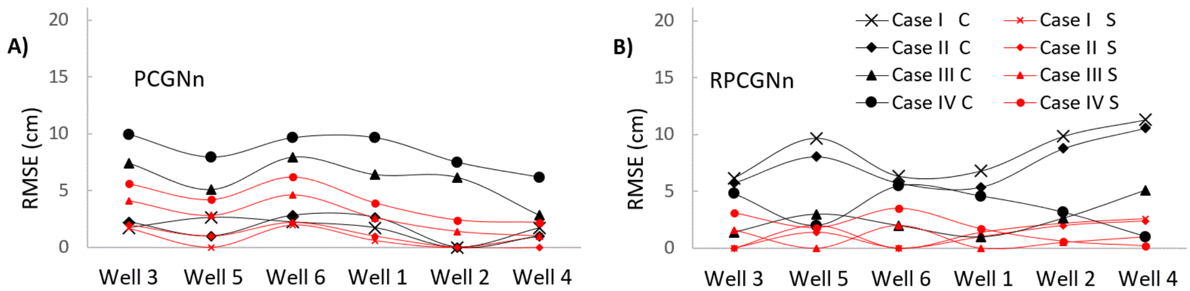

***Fig. 5** Grid effect on a) PCGNn and b) RPCGNn models with respect to well location, for all drawdowns. C stands for cumulative and S for small, indicating the range of drawdowns included in RMSE calculations*

RPCGN1 always produces unfavorable results for Wells 2 and 4 (at and the closest to the center), regardless of the global grid used. With coarser global grids, Wells 3 and 6 (wells closest to the constant head boundary) outputs acceptable results; when 51x51 is used, Wells 3, 5, 6, and 1 (closest to the boundary) provides better results; and with 77x77, 5 and 1 generate better. With RPCGN100, Well 6 produces higher $RMSE$s with all global grids while Well 5 provides somehow acceptable close-results for all grids (Table 5).

For small discharge rates, the $RMSE$s are mostly considerably small, except the bolded ones in Table 5 (only two exceptions to this took place with finer grids (*cases III* and *IV*) for PCGN100 and PCGN1 models, in Wells 4 and 5, respectively). Cumulative $RMSE$s for PCGN1 and RPCGN1 are highly larger than that of smallest two drawdowns. For PCGNn, *cases III* and *IV* produce large differences, while for RPCGNn and RPCGN100 in *cases I* and *II* the results largely differ according to the discharge rate.

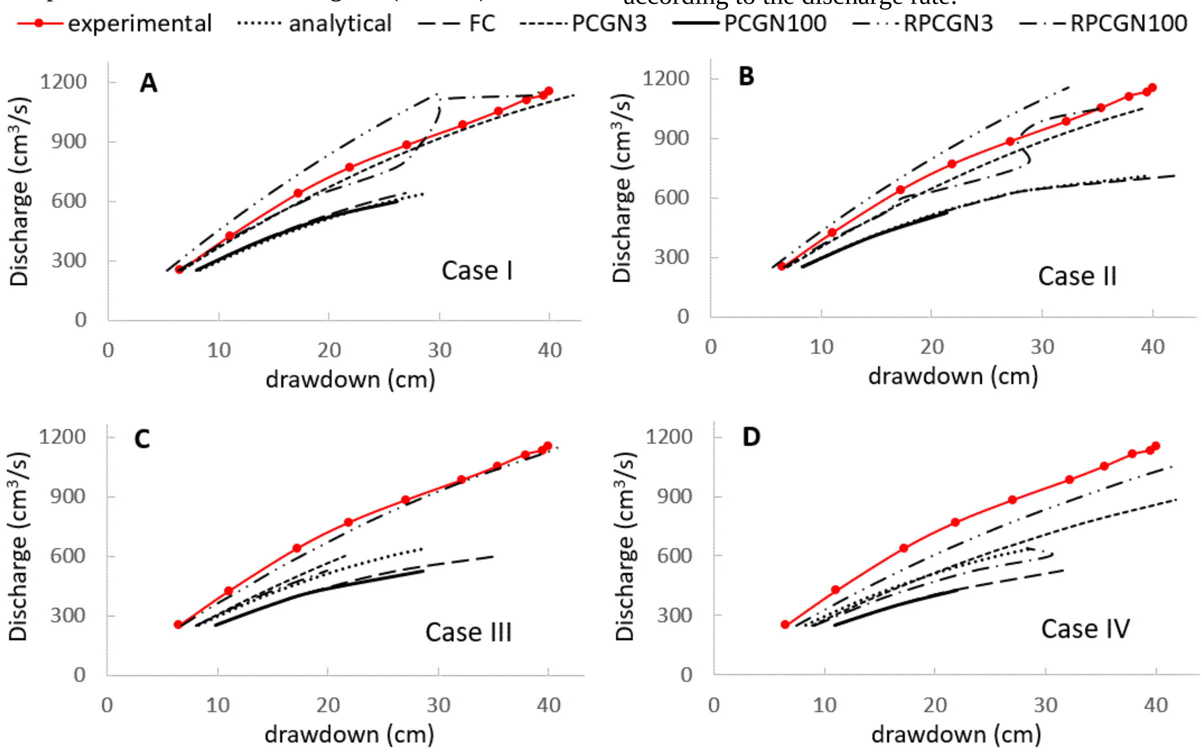

***Fig. 6** Discharge-drawdown relationships for well 1 in all four implemented global grids: a) case I; b) case II; c) case III; and d) case IV. Linear models were left out for clarity.*

Fig. 6 shows that, as the grids get finer in spacing, the solutions produce increasing drawdowns; this is consistent with all wells and numerical solutions. Therefore, if the solutions overestimate the drawdowns, the spacing should be increased, and if the solutions underestimate, with finer mesh the results become more consistent, as in RPCGNn (Table 5; Fig. 5b; Fig. 6).

Overall, methods are mesh-sensitive as for which gives better results and this also changes with well position. Almost without any exception, PCGNn provides the best results for coarser uniform grids and RPCGNn for the finer. Other techniques perform better with some wells than others. For *case I*, drawdowns in wells close to the center (Wells 4, 2, and 1) of the circular aquifer may be predicted using PCGN100, FC, and analytical and for wells far from the center using PCGN1, RPCGN1, RPCGN100, and RPCGNn. For *case III*, PCGN100 and FC (as in *case I*) provides good results at and around the center and diverges from the experimental when the wells are located within the outer half of the aquifer diameter; unlike *case I*, analytical solution will not follow them. In wells closer to the constant head boundary, RPCGN1 performs better as in *case I*; nonetheless, PCGN1 and RPCGN100 give less accurate results in *case III* when compared to *case I*. For *case IV*, too, PCGN100 provides small $RMSE$s for the center well and the RMSE increases gradually as the location of the eccentric wells lie near the boundary. The increase in error is also true for FC, which is grossly overestimating the drawdowns in Well 3 for the only two discharge rates, 428.57 and 618.57; it produces output that but not for the analytical. RPCGN1, on the other hand, does not have a consistent change in *case IV*; it is good for Wells 1 and 5.

Discussion and conclusions

The results of this study reveal that smaller drawdowns provide more consistent results for wells eccentrically located in a circular island unconfined aquifer. The degree of this consistency, however, differs among the models with refinement and discretization. With respect to mesh size, some methods perform better than others do for a certain mesh. PCGN solver with user controlled *iter_mo* adapts to finer grids if local refinements at and around the well are performed (RPCGNn); however, the explanation to this condition is not clear. Generally too-fine mesh is not considered due to its consumption of computer memory and computation time; studies such as in Rushton and Tomlinson (1977) gear towards using coarser grids permissible to obtain optimal results. Well eccentricity matters in terms of global grid selection: wells closer to the aquifer center are more likely to produce robust outputs.

Overall, there is no need for excessive refinement or fine discretization as long as a single well operates; thus, *case I* and *case II* adequately address the problem at hand. However, if for any reason, local refinement is needed, the global mesh must be finer for consistency. In conclusion, if the geometry of the model changes, the mesh sensitivity analysis should be conducted in order to choose the optimal grid.

Our data showed that, for most models, numerical results gradually deviate from experimental results as the eccentricity of the well in operation increases. This is only logical because, for example, the distance from the external circular boundary dwindles to 25 cm for Well 3, which, in turn, contradicts the Dupuit's assumption that the aquifer is infinite and because the large vertical flow components (for Well 3, a drawdown of 38.1 cm is obtained experimentally while 25 cm afar the drawdown is zero). This also confirms the results that, for smaller drawdowns, $RMSE$s are smaller because only in those cases do the theoretical and physical models become more in line with each other.

The discharge rate should not be any larger than when the oscillations in Fig. 3 start taking place in order for PCG2 (or PCGN100) to be used. For Well 4, for example, it should not go roughly beyond 570 cm^3/s after which large drawdown fluctuations occur before the convergence (for a smaller than experimental drawdown) takes place. The high $RMSE$s for the FC (and perhaps for PCGN100 (or PCG2)) emerge due to overestimation of drawdowns for these models, something expected because at high discharges the vertical gradients create seepage face, something the Dupuit assumptions preclude, and the assumption that no flow through the vadose zone takes place.

Picking an iter_mo that is not big enough for the PCGN solver to converge is a questionable step to take. One may also argue that for finer global grids the results do not reflect that of experimental if refinement is not applied. The response to that would lie in the fact that the used *iter_mo*s were calibrated under the coarser grids. Thus, knowing that *iter_mo* depends on eccentricity, and it adapts to the discretization, it is an innovative way to deal with the problem of overestimated drawdowns in converged cases (PCG2 and PCGN100). Therefore, it is suggested that, as long as there is large drawdown data to calibrate the model, working with non-converged models is acceptable, and, thereby, verifies that MODFLOW's PCGN solver may be used in circular island unconfined aquifers for eccentric wells as long as it is user-controlled. The same conclusion cannot be stated for PCG2 solver unless either the drawdowns or the eccentricity is small.

Another challenge in this study was regarding the drying cells. Through refinement of well itself, this was minimized, in that, while the head at some cells within the well dropped below the aquifer base, some still remained above, and when averaged, the drawdown remained above zero. Future studies may include changing the default parameters used in this study to examine how well the converged results perform.

The results of this study indicated that the PCGN solver performs well in drawdown estimation for eccentric wells in Circular Island unconfined aquifers under steady state condition provided that calibration data for high drawdowns is available. PCG2 and PCGN100 provide the same outputs for same grid systems. PCG2 and FC models' performance is limited to small drawdowns and small eccentricities, and they gradually diverge from the experimental when either of them becomes larger. Analytical model performs well for very small eccentricities. This is coherent with the fact that wells closest to the outer boundary perform better with PCGN1 (linear solution) and closer to the center with PCGN100, showing that less eccentricity means more nonlinearity. For single-well operating systems, models perform better using course grids.

However, the overlap of the analytical, FC, and PCGN100 results, and the obvious error in some of the experimental measurements (the unreasonable results of Well 5) may lay a ground to replicate the experiments for a well-grounded conclusion. The findings in this study may be of practical uses in pump and treat systems designed to prevent contamination from spreading or remove contaminant mass in unconfined aquifers. This could be achieved by controlling the discharge rate and the drawdowns.

References:

1. Birpinar, M. E., & Gazioglu, S. A. (2002). Discharge-drawdown relationship of eccentric wells. *Journal of Hydrologic Engineering, 7*(3), 260-264.

2. Babbit, H., & Caldwell, D. (1948). The free surface around, and interface between, gravity wells. *Engineering Experiment Station.*

3. Boulton, N. S. (1951). The flow pattern near a gravity well in a uniform water-bearing medium.(includes appendices). *Journal of the Institution of Civil Engineers, 36*(10), 534-550.

4. Clement, T., Wise, W. R., Molz, F. J., & Wen, M. (1996). A comparison of modeling approaches for steady-state unconfined flow. *Journal of Hydrology, 181*(1), 189-209.

5. De Wiest, J. R. (1963). Flow to an eccentric well in a leaky circular aquifer with varied lateral replenishment. *Geofisica Pura E Applicata, 54*(1), 87-102.

6. Dupuit, J. (1863). *Etudes theoriques et pratiques sur le mouvement des eaux dans les canaux decouverts et a travers les terrains permeables avec des considerations relatives au regime des grandes eaux, au debouche a leur donner et a la marche des alluvions dans les rivieres a fond mobile* Dunod.

7. Hantush, M. S. (1964). Hydraulics of wells. *Advances in Hydroscience, 1*, 281-432.

8. Hantush, M. S., & Jacob, C. E. (1960). Flow to an eccentric well in a leaky circular aquifer. *Journal of Geophysical Research, 65*(10), 3425-3431.

9. Mishra, P. K., & Kuhlman, K. L. (2013). Unconfined aquifer flow theory: From dupuit to present. *Advances in hydrogeology* (pp. 185-202) Springer.

10. Muskat, M., & Wyckoff, R. D. (1937). Flow of homogeneous fluids through porous media.

11. Rushton, K. R. (2003). *Front matter* Wiley Online Library.

12. Rushton, K., & Tomlinson, L. (1977). Permissible mesh spacing in aquifer problems solved by finite differences. *Journal of Hydrology, 34*(1-2), 63-76.

13. Shamsai, A., & Narasimhan, T. (1991). A numerical investigation of free surface—Seepage face relationship under steady state flow conditions. *Water Resources Research, 27*(3), 409-421.

14. Siddiraju, S. (2013). Pumping test analysis of large diameter wells in pulang river basin cuddaph district. *International Journal of Innovative Research and Development|| ISSN 2278–0211, 2*(3), 129-136.

15. Verruijt, A. (1982). The finite element method. *Theory of groundwater flow* (pp. 105-121) Springer.

16. Wang, H. F., & Anderson, M. P. (1995). *Introduction to groundwater modeling: Finite difference and finite element methods* Academic Press.